Nuclear Instruments and Methods in Physics Research B 546 (2024) 165160

Contents lists available at ScienceDirect

Nuclear Inst. and Methods in Physics Research, B

journal homepage: www.elsevier.com/locate/nimb

Effect of irradiation and chemically aggressive environment on Brazilian mortar cement

Fabiano Yokaichiya [a], Eduardo A.G. Ferreira [b], Roberto Vicente [b], Augusta Cerceau [c], Júlio T. Marumo [b], Margareth K.K.D. Franco [b,*]

[a] Universidade Federal do Paraná – UFPR, Brazil
[b] Instituto de Pesquisas Energéticas e Nucleares –IPEN, Brazil
[c] Universidade Federal de Minas Gerais- UFMG, Brazil

ARTICLE INFO

Keywords:
Cement
X-ray tomography
X-ray diffraction

ABSTRACT

Radioactive waste disposal, considered a major technical problem, has as one of the solutions, the construction of repositories that will be exposed to a range of environmental conditions in a timescale which involve thousands of years. Cement-based materials, used in the repositories, have a complex porous structure that changes over time and their durability strongly correlates to the transport of water and ions throughout the pore structure. In this study, the influence of the repository's environment was simulated using two different solution conditions: Water and Na_2SO_4 at different gamma irradiated condition. Two X-Ray techniques were performed simultaneously: (i) diffraction to characterize the phases contents on cement mortar samples; (ii) tomography to investigate the differences between the pore structure and pores volume. The combination's advantage of the X-Ray techniques shows their potential application to determine the relation amongst the phases and the pores structures, to demonstrate how the environment and the irradiation modify the structure of mortar.

1. Introduction

Radioactive waste has been generated increasingly in many countries as increases the demand for nuclear applications in medicine, agriculture, research and industry, including power production. Producers of radioactive waste also includes a number of activities such as the operation and decommissioning of nuclear facilities; the remediation of contaminated sites; and the processing of ores containing naturally occurring radionuclides.

The importance of the safe management of radioactive waste including disposal for the protection of human health and the environment has long been recognized, and substantial knowledge has accumulated worldwide. Radioactive waste management is always designed as a series of treatment and conditioning operations aimed at reducing the volume and producing a waste form that meets the requirements for safe, long-term disposal [1–3].

The special category of radioactive waste that is composed by the disused sealed radioactive sources requires a disposal technology that brings together characteristics of the low- and intermediate-level waste and of the high-level waste. Some sources have very long-lived radionuclides and possesses high enough activities to require higher levels of containment and isolation that cannot be provided by near surface disposal facilities, implying the need for disposal at greater depths. The disposal options comprise repository components that will be subjected to a range of environmental conditions in a timescale which involve hundreds or thousands of years.

In order to assess and predict repository behavior and performance over this large time-scales, it is essential to have good knowledge and understanding of the behavior of different materials to form a technical basis for establishing disposal facilities prior to for waste immobilization, as well as for engineered barriers associated with storage and disposal facilities for their long-term isolation from the biosphere.

Present in waste forms, packages and backfills, cement materials contribute to mechanical stability and support at both storage and disposal stages. Cement has a high pH and forms hydration products being a durable solid material with a low permeability in its hardened state, which isolates the radioactive waste, facilitating its safe transportation and storage [4].

However, the repository environment can affect and degrade the engineered barriers of waste storage and disposal facilities. The slow but

* Corresponding author.
E-mail address: margareth_franco@yahoo.com.br (M.K.K.D. Franco).

https://doi.org/10.1016/j.nimb.2023.165160
Received 8 August 2023; Received in revised form 1 November 2023; Accepted 6 November 2023
Available online 10 November 2023

continuous degradation process generated by exposure to such environmental factors as ionizing radiation and aggressive chemicals dissolved in groundwater, after the cement hardening period, can affect its integrity during the lifetime of the repository [5–8]. For instance, the - formation of Ettringite that evolves from exposure to chlorides, carbon dioxide and sulfates, result in various chemical degradation phenomena, such as microstructural alterations [9].

The Radioactive Waste Management Department at Nuclear and Energy Research Institute (IPEN-CNEN/SP), São Paulo, Brazil, is developing the concept of a disposal facility for the disused sealed radioactive sources, known as deep borehole. This facility could offer the prospect of disposal at a reasonable cost, on the scale accessible to non-nuclear countries while, at the same time, meeting all the safety requirements for disposal of long-lived sources with very high activities [10].

The IPEN borehole concept is a steel pipe about 20 cm in diameter and 400 m long that will be placed as the casing of a borehole drilled in a crystalline rock formation, the space between the rock and the steel being backfilled with cement paste, in order to make a rigid structure and impeding any movement of water between the different strata of the geological setting. The sealed sources will be disposed of at the bottom of the borehole, inside specially-built, steel containers, up to a height of approximately 100 m. The space from the top container to the surface will be filled with concrete, to prevent or hinder access to the sources in the future.

As in any other disposal facility, the long-term behavior of the components of the borehole structure must be assessed in order to give reasonable assurance of the safety of people and environment, in this case for thousands of years. Investigations are being conducted to evaluate the durability of the components such as the metallic structures and the cementitious materials. Cementitious materials hydrates may be unstable in the long term, as their mineralogy and microstructure can change over time, due to: (i) recrystallization of the cement gel or (ii) the chemical reaction with aggregates and substances in the environment. Hydrated cement, in the environment of a deep repository, will be exposed to higher temperatures and pressures, aggressive chemicals dissolved in groundwater and the radiation field of discarded waste, negatively affecting its durability, inducing changes in mineralogy and microstructure, thus increasing porosity and reducing mechanical strength. For these reasons the aim of this study is to evaluate, through accelerated degradation experiments in laboratory, the behavior of cement-based materials under potentially aggressive environments, as expected in the prospective geological disposal environments of Brazil.

In this study, using X-ray diffraction and tomography techniques simultaneously, we were able to: a) Identify mineralogical and structural changes in cementitious materials when immersed in sulphate solutions prepared in laboratory; b) Evaluate mineralogical and structural effects of irradiation in cement-based materials. Our research has demonstrated, through the combination of X-ray techniques (X-ray diffraction and X-ray microtomography), that it is possible to determine the relationship between phases and pore structures in the mortar structure, when subjected to different environmental and the irradiation.

2. Materials and methods

2.1. Sample preparation

Cement mortar samples (CMS) were exposed to gamma radiation source and to sodium sulphate solution/water in order to simulate a potentially aggressive environment of a deep borehole repository. Samples were made with Portland cement type II-Z (CPII-Z) [11], Brazilian standard sand (ABNT NBR 7214) [12], superplasticizer MC-Power Flow 400 (Bauchemie) and distilled water. Water to cement and cement to sand ratios was 0.5 and 1.0, respectively. CPII-Z has 6–14 % of pozzolan content and it was chosen to be the most similar to the CEM II B-V 32.5 N, recommended by the International Atomic Energy Agency. Superplasticizer is used to extend the workability and allow the pumping into deep wells.

Table 1
Exposure conditions of the samples in the degradation experiments. NI-.non-irradiated sample, IR-irradiated sample.

Sample	Storage conditions	Irradiation
NI-201	Nitrogen	0 MGy
NI-211	Sodium Sulfate [1 M]	0 MGy
NI-213	Water	0 MGy
IR-801	Nitrogen	0,2 MGy
IR-811	Sodium Sulfate [1 M]	0,2 MGy
IR-813	Water	0,2 MGy

Cylindrical samples (3.0 x 2.5 cm, height x radius) were withdrawn from one sample molded in an aluminium tray (3 x 18 x 27 cm (height x width x length) in order to guarantee their homogeneity. The sample molded in a tray was previously kept for 28 days in curing chamber with 99 % of relative humidity, at 21 °C. Submerging the samples in acetone was the methodology used to interrupt curing. They remained stored in the desiccator at a temperature of 21 °C until characterization measurements were carried out. Degradation experiments were conducted with 2 mm thickness discs obtained from cutting the cylindrical samples with a Buehler Isomet 1000 precision sectioning saw. Then, all faces of the discs were covered with epoxy resin leaving 1 cm^2 window uncovered. This procedure allowed only a small opening for water penetration during immersion, thus obtaining a reaction front from the surface of the samples towards the centre, necessary to avoid the fast reactions on the surface of the samples.

CMS were cast and, after the curing time, exposed to accelerated degradation experiments, simulating a potentially aggressive environment of a deep borehole repository. The CMS were exposed to: (i) a gamma radiation source, 0,2 MGy and (ii) immersion in salt solutions containing sulphate ions or in distilled water at 20 °C. A summary of the exposure conditions is shown in Table 1.

The samples subjected to irradiation were taken to a 60-Co irradiator with 3,408TBq of activity and maximum dose rate of 15 kGy/h, at the Ciclotron Accelerator Center (CAC), at IPEN-CNEN/SP. The irradiation aimed to simulate the dose accumulated by the radiation field present in a borehole for sealed radioactive sources, considering the doses corresponding to those deposited by the most intense and relevant discarded sealed radioactive sources in the Brazilian inventory, of 137Cs, 226Ra and 241Am-Be. The samples were irradiated until a dose of 1, 2, 3, 4, 5, 8 and 10 MGy (megagray) was accumulated.

2.2. Experimental characterization techniques

The X-ray Diffraction and micro tomography measurements were performed simultaneously on the 7T-MPW-EDDI beamline: Energy Dispersive Diffraction Beamline, in BESSY II, Berlin-GE [13]. The phases in the sample were obtained by analyzing X-Ray diffractograms using Rietveld refinements. TOPAS software was used to refine the diffractograms obtained by X-Ray Diffraction analysis, using pre-determined phases. The phases used to refine the diffractograms were: tricalcium silicate (Alite), dicalcium silicate (Belite), Portlandite, Periclase, Quartz, Calcite, Celite, Celite H, Lime, Brownmillerite, Ettringite and the CSH gel.

The pore structure of the cement paste samples was investigated by X-ray micro tomography(μCT). This technique allows to analyze the total volume and the porous volume present in a given sample. In this way, it is possible to evaluate the porosity of the selected sample. The reconstruction of the μCT 3D images were performed using Avizo® software and software Octopus® V 8.6, which was based on a back-projection algorithm with convolution and correction for cone beam.

Table 2
The Rwp, gof and cimentitions phases contents. The results are normalized for the quartz content, for the non-irradiated mortar sample (NI) and the irradiated mortar sample (IR).

Sample	NI-201	NI-211	NI-213	IR-801	IR-811	IR-813
r-wp	16,0	18,3	14,2	14,4	16,0	13,8
gof	1,77	2,17	1,62	1,71	1,79	1,47
Alite [%]	1,3	0	0	0	2,06	0,52
Belite [%]	12,3	17,6	19,5	2,78	24,5	10,6
C4AF[%]	2,94	1,42	0,89	1,65	11,6	12,7
Lime [%]	0	0	0	0	1,05	0,67
Portlandite [%]	3,51	13,2	10,9	0,99	13,2	4,52
Periclase [%]	0,02	0	0	0	0	0,35
Calcite [%]	63,8	28,3	25,7	50,8	18,7	29,4
Celite [%]	2,05	0,44	0,7	0,39	14,1	10,8
Tricalcium DiAluminium Hidroxide [%]	0,07	24,7	28,5	0,24	0,05	0,29
Ettringite [%]	11,9	0,6	1,8	40	11,3	9,02
CSH-gel [%]	2,03	13,8	11,9	3,14	3,43	21,2

3. Results and discussions

3.1. X-ray diffraction

In order to characterize multiphase system and to refine a theoretical profile, Rietveld refinement gives, using TOPAS software [14], a series of parameters to verify the calculated and measured profiles matching. Amongst the refinement parameters, goodness of fit (gof), is the ratio between the weighted-profile (Rwp) and the expected-profile (Rexp). The ideal gof is one, however in multi-phases systems, like cimentitious materials, the gof might be much higher.

Table 2 shows the XRD results of Rwp, gof and cimentitions phases for the specimens (NI – not irradiated and IR – irradiated) that were kept in dry storage and maintained in a nitrogen atmosphere, to avoid the formation of calcite on the surface. Fig. 1 and Fig. 2 display the refinement of diffractograms of NI and IR mortar samples in Na_2SO4 solution or water respectively.

Comparing the samples in water, NI and IR, the results obtained showed that the applied gamma irradiation did not change considerably in the set of hydrates phases. However, it is clear that there was dehydration induced by radiation observed indirectly by 3 indicators: (i) the 10 % increase in the amount of CSH (11.97 % to 21.15 %), (ii) the 7.22

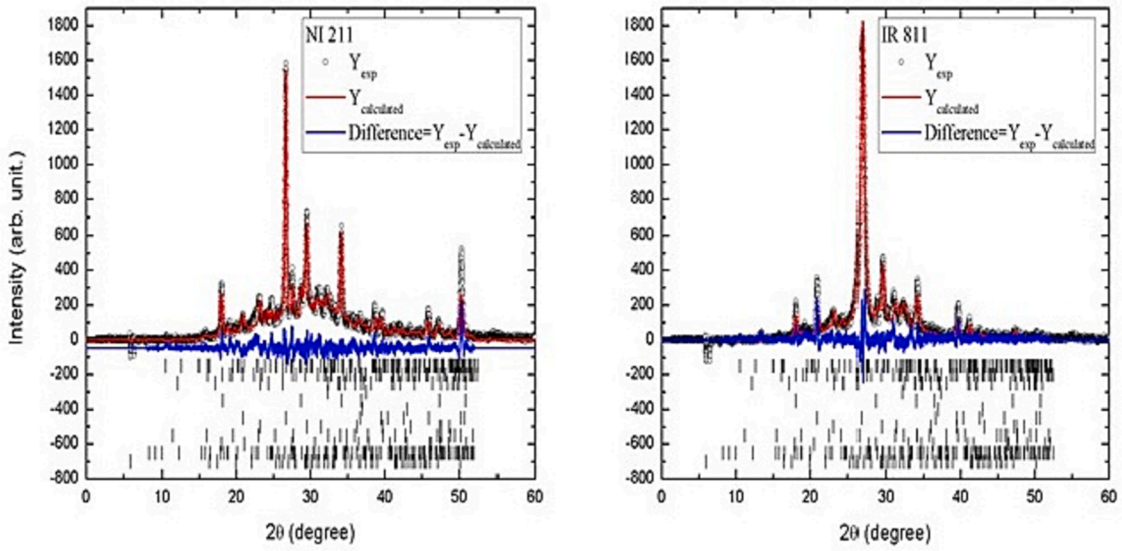

Fig. 1. Diffractogram of NI-211 and IR-811.

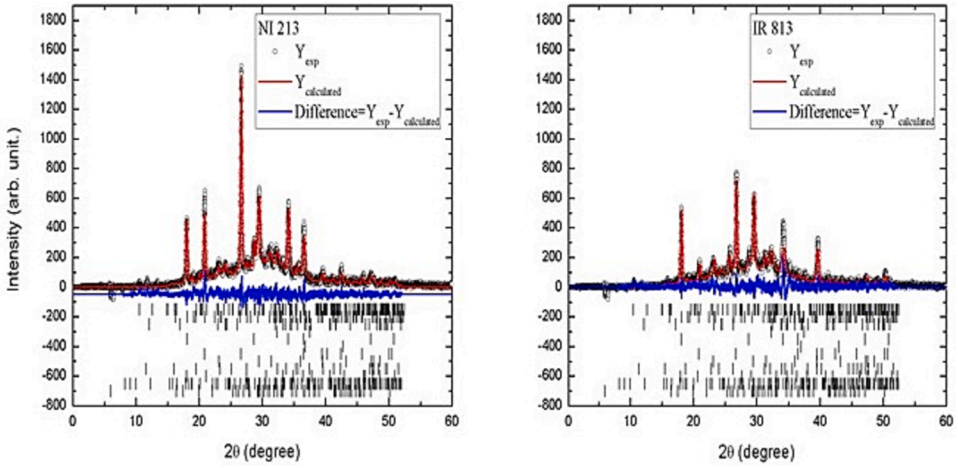

Fig. 2. Diffractogram of NI-213 and IR-813.

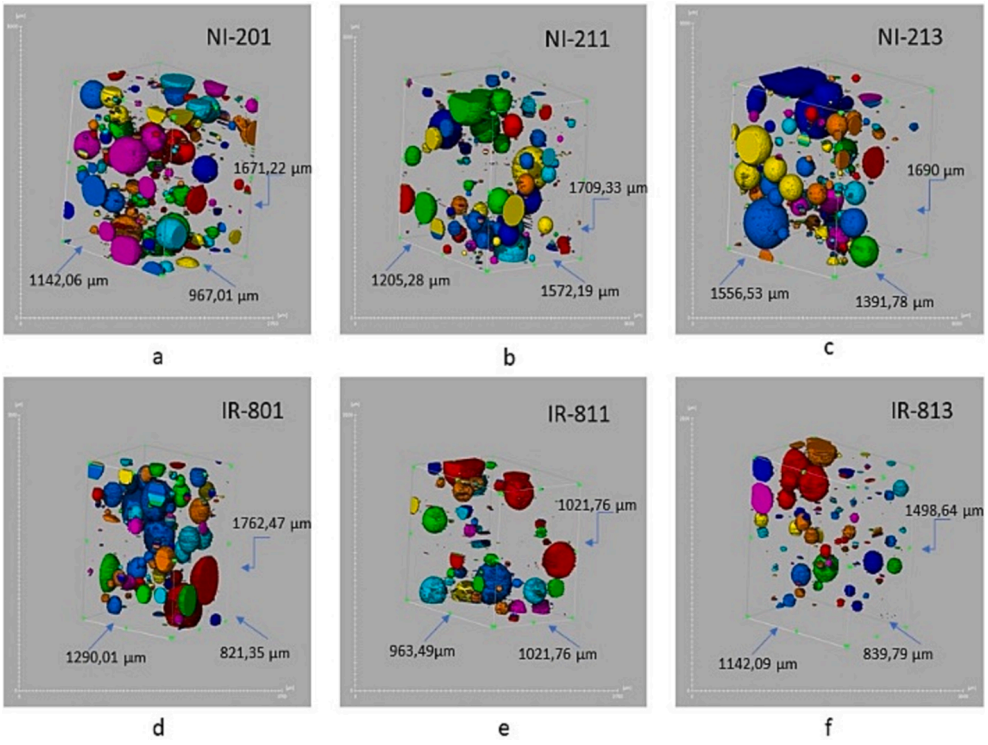

Fig. 3. Reconstructed µCT images of NI and IR samples.

% increase in the amount of Ettringitte (1.8 % to 9.02 %) and (iii) the 8.19 % decrease in the amount of Alite + Belite (19.49 % to 11.3 %). Moreover, the decrease of the Portlandite amount from 10.93 % to 4.52 % is also a result due to irradiation of samples in water.

In addition, the decrease in Tricalcium dialuminium hydroxide phase from 28.49 % to 0.29 % contributed to the increase of Celite phase from 0.7 % to 10.75 % and the increase of Etringitte phase from 1.8 % to 9.02 %. The radiolysis [15,16] of water caused by radiation accelerated Belite's reaction, in which its natural state is slower than its polymorph Alite. We observed an increase in the amount of Calcite phase from 25.73 % to 29.41 % for the irradiated samples. These results are in agreement with the work of Vodák et al. [17] and Bar-nes et al. [18], in spite of the irradiation value being lower than those applied by the researchers.

Comparing the dry sample, NI and IR, we observed an increase of Ettringite production from 11.94 % to 40 % when irradiated, and a decrease in Alite + Belita from 13.63 % to 2.78 % when irradiated. These results suggest that the radiolysis in the confined water provokes the continuity in the degradation reactions of Alite + Belite. Regarding Celite, Portlandite and Brownmillerite phases we observed the decrease of their amounts, indicating that radiation provides the formation of Ettringite.

Comparing the samples in Na_2SO_4 solution, NI and IR, we notice a decrease in CSH-gel from 13.81 % to 3.43 %, and a decrease in Tricalcium dialuminium hydroxide from 24.65 % to 0.05 % caused by water radiolysis. Tricalcium dialuminium hydroxide phase decrease justifies the Celite phase increase from 0.44 % to 14.14 %, the Etringite phase increase in from 0.6 % to 11.32 % and the Brownmillerite increase in from 1.42 % to 11.6 %. Portlandite showed no significant change. The reversibility reactions (Eqs. (1.1) to (1.3)) [19,20] that lead the dissolution-formation of (Alite + Belite) to (Portlandite + CSH) justify the increase in the amount of Belita from 17.61 % to 24.5 %, and Alita from 0.00 % to 2.00 %.

$$C3S + 3H2O \rightleftarrows 3Ca^{2+} + H2SiO4^{2-} + 4OH^{-} \quad (1.1)$$

$$C2S + 2H2O \rightleftarrows 2Ca^{2+} + H2SiO4^{2-} + 2OH^{-} \quad (1.2)$$

$$Ca2 + + H2SiO4^{2-} + 2(x-1)OH^{-} + yH2O \rightleftarrows xCaO.SiO2.yH2O \quad (1.3)$$

Comparing NI samples in water and in Na_2SO_4 solution (0.1 Molar), we perceive that the sulfate in the solution does not influence the Ettringite formation in our studies. Nonetheless, in the case of IR samples, we are able to detect a small increase in Ettringite from 9.02 % (in water) to 11.32 % (in Na_2SO_4 solution), but a remarkable decrease in CSH from 21.15 % to 3,34 % [21]. These results suggest that the incorporation of the sulfate solution by the samples, when expose to gamma radiation, cause the release of sulfate ions in the cementitious matrix [22,23].

3.2. X-ray tomography

X-ray tomography technique has proven to be a powerful non-destructive technique to investigate cementitious materials as a direct visualization of the porous structure distribution and pores volume, while X-ray diffraction provided important insights regarding the structure.

In this study, µCT provides us an insight into the structure of these complex cementitious material systems. We explore 3D imaging and its interpretation that allows us a better understanding concerned to its pore distribution (porosity).

Fig. 3 show the reconstructed µCT images of NI and IR samples. It is clearly observed differences in the numbers of pores of the images.

In mortar cement, the pores vary in size, shape and origin. They are subdivided in the following classes: (i) Pores in the cement paste matrix (gel pores, capillary pores, hollow shell pores and air voids), (ii) Pores in aggregates, (iii) Pores associated with the interface between aggregates and cement paste matrix, (iv) Voids with water and (v) Internal discontinuities in the cement paste matrix associated with dimensional instabilities that occur during changes in humidity and temperature [24]. In our study we will pay attention to the hardened cement paste matrix pores, focusing on capillary pores, empty shell pores and air

Table 3
Pore diameter dimension classification according to Aligizaki [24].

Pores	Diameter dimensions
Pores: gel	$4.10^{-4} - 10^{-3}$ μm
Pores: capillary	Meso Poros $10^{-3} - 5.10^{-1}$ μm, Macro Poros 5.10^{-1}-10 μm
Pores: empty shell pores and air voids	10–100 μm

voids.

The pores analyzed in this study by the tomography method, which according to Young [25] is classified as Capillary Pores – Macro pores, will be defined as empty pores, due to their origin, according Table 3.

Fig. 4 displays an example cross sectional slice image of a cement sample NI-211, where high contrast provided by the high flux synchrotron x-rays is illustrated. One can see pore spaces (dark spots in the image detailed, as labeled in the image). The image clearly highlights the microstructure and its heterogeneity.

Table 4 displays the quantitative treatment of the images that reveal the total number of pores and total volume of voids.

According to Table 4, the number of pores substantially decreases (around 50 %) due to irradiation when the sample was submerged in water, from 354 (NI-213) to 154 (IR-813) pores air voids and from 74 (NI-213) to 27 (IR-813) capillary pores. These results clearly show the strong contribution of the aqueous medium subjected to irradiation. Thus, the sample in the aqueous medium analysis suggests that the radiolysis promotes capillary pore junction, as observed in the literature [26,27]. Comparing samples submerged in water (NI-213) and in solution (NI-211), the number of pores is practically the same. However, we observe a decrease in the number of air voids pores from 411 to 260 and capillary pores from 91 to 58, in samples in solution, non-irradiated and irradiated respectively (NI-211 and IR-811).

Fig. 5 shows the histograms of the pore number distribution as a function of the pore radii of the NI samples at 201, 211, 213. In the analysis of NI samples, two types of pores were observed: Macropores-Capillary pores (empty pores) and Macropores-Air Voids. We note that $NP_{NI201} > NP_{NI211} > NP_{NI213}$.

When the detailed histograms (Fig. 5b, d and f) are analyzed, we verified that the macropores-capillary pores in the dry sample show a regularity in the number of pores as a function of the porous radius. On the other hand, the samples in Na_2SO_4 solution and in water present a higher concentration of the number of pores in the range of 10 μm to 12 μm in radius.

Fig. 6 shows the histograms of the pore number (NP) distribution as a function of the pore radii of the IR samples at 801, 811, 813. In the analysis of IR samples, two types of pores were observed: Macropores-Capillary pores (empty pores) and Macropores-Air Voids. We note that $NP_{NI801} > NP_{NI813}$ while $NP_{NI811} > NP_{NI801}$ (Table 4).

When we analyzed the detailed histograms (Fig. 6b, d and f) we verified that the macropores-capillary pores in the water sample presented a regularity in the number of pores as a function of the radius, while the dry samples and in Na_2SO_4solution presented a higher concentration of the number of pores in the range of 10 μm to 12 μm in radius.

Fig. 7 shows the analysis of the pore surface-volume ratio versus the pore radius for the various observed conditions. Considering a fixed volume, the sphere is the geometric shape that has the smallest surface (ratio SV = 3/pore radius) represented by the red curve, and the

Table 4
Total pores number and average pore size of samples.

Samples	Types of pores	Total number of pores	Average pore volume [μm^3]	Standard Deviation [μm^3]	Total pore volume [μm^3]
NI-201	Capillary pores	98	8117,35	7781,30	795500,00
NI-201	Air voids	480	389030,95	282809,47	186735000,00
NI-211	Capillary pores	91	7526,10	7794,20	684875,00
NI-211	Air voids	411	35174,94	266539,52	146799000,00
NI-213	Capillary pores	74	6658,78	6624,09	492750,00
NI-213	Air voids	354	381385,95	254139,98	135011000,00
IR-801	Capillary pores	29	5556,03	4745,84	161125,00
IR-801	Air voids	218	360396,31	234222,31	78566400,00
IR-811	Capillary pores	58	5657,33	5616,22	328125,00
IR-811	Air voids	260	386326,98	262978,65	100445000,00
IR-813	Capillary pores	27	9629,63	8933,08	260000,00
IR-813	Air voids	154	360789,45	260812,06	55561600,00

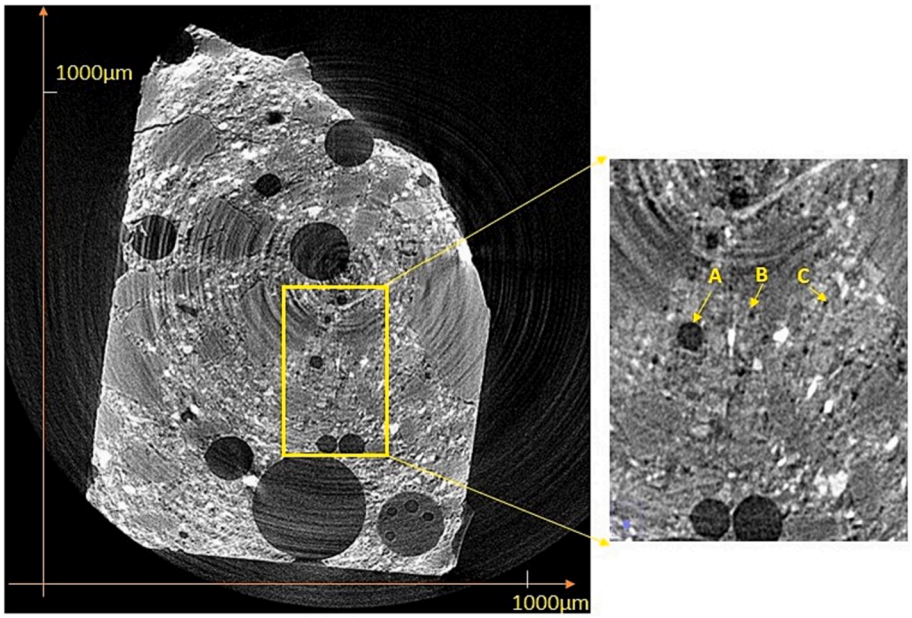

Fig. 4. (Left) Cross sectional slice image of a cement sample NI-211, and (Right) highlights detailed showing 3 pores diameters: A (1000 μm), B (25 μm) and C (5 μm).

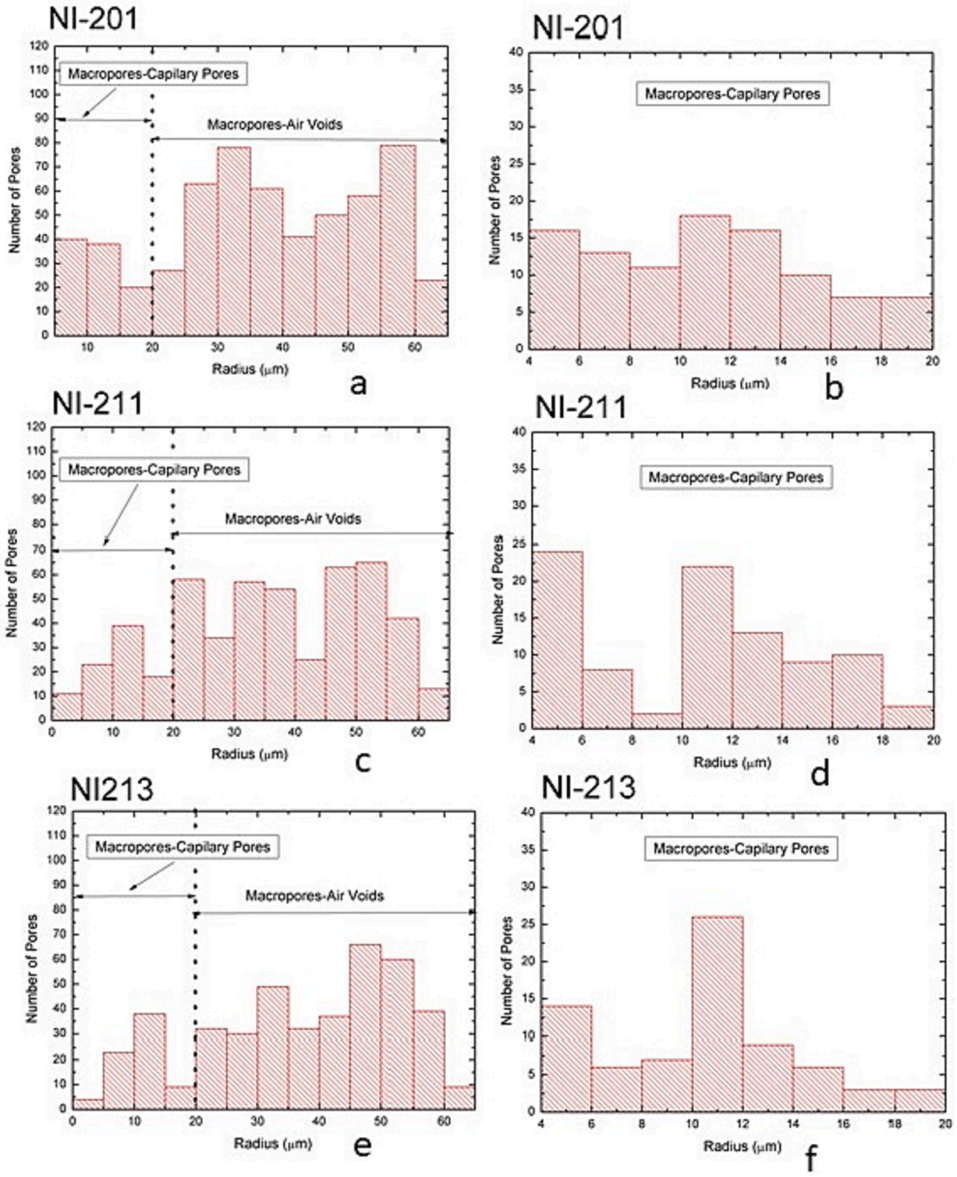

Fig. 5. Pore number (NP) distribution histograms of the NI samples.

tetrahedron the largest surface among the regular shapes (non-fractal, ratio SV = 14.697/Pore radius) represented by the blue curve in the Fig. 7. Points located between these curves have regular (non-fractal) surfaces. We observed in all cases (Fig. 7a, 7b, 7c) that pores with radii smaller than 20 μm (macropores-capillary pores) present S-V ratio values between 1000 and 10, indicating high fractality. For air voids (radius greater than 20 μm) the S-V ratio presents values lower than 10, indicating low or even non-fractality.

4. Conclusions

In this study it is clearly demonstrated that the potential application of X-ray microtomography 3D imaging combined simultaneously with x-ray diffraction technique, provides us an overall view of phases composition associated to porous structure of cimentitious materials applied to repositories construction, to show that the gamma radiation and aggressive Na_2SO_4 solution modified the pore structure and the chemical compositions of the cement samples.

Although the connection between the X-ray CT and XRD is not direct, since the phase composition changes may not result in pore size distribution changes, this complementarity allowed us to verify the complete range of pore dimensionality from pores gels, indirectly observed, through X-ray diffraction, related to the amount of CSH, to capillary macro pores and air voids, observed directly by x-ray microtomography.

The results concerned the amount of CSH show that dry samples do not change when irradiated, not modifying the amount of gel pores. However, the amount of CSH in water samples increased from 11.97 % to 21.15 %, indicating an increase in the number of gel pores, while samples in sulfate solution reduced from 13.81 % to 3.43 %, implying a decrease in the amount of gel pores. On the other hand, the number of capillary pores and air voids decrease when irradiated for all the cases, as shown via x-ray microtomography. These behavioral differences amongst pores gels, capillary pores and air voids, can be explained by their origins. Pore gels are indirectly related to CSH amount, that is affected by water radiolysis through the irradiation. Differently, capillary pores and air voids are affected to the irradiation but not connected to CSH amount. Concerning the fractality analysis, obtained via X-ray microtomography by calculating S-V ratio, we observe, in all the samples, that pores with radii smaller than 20 μm (macropores-capillary

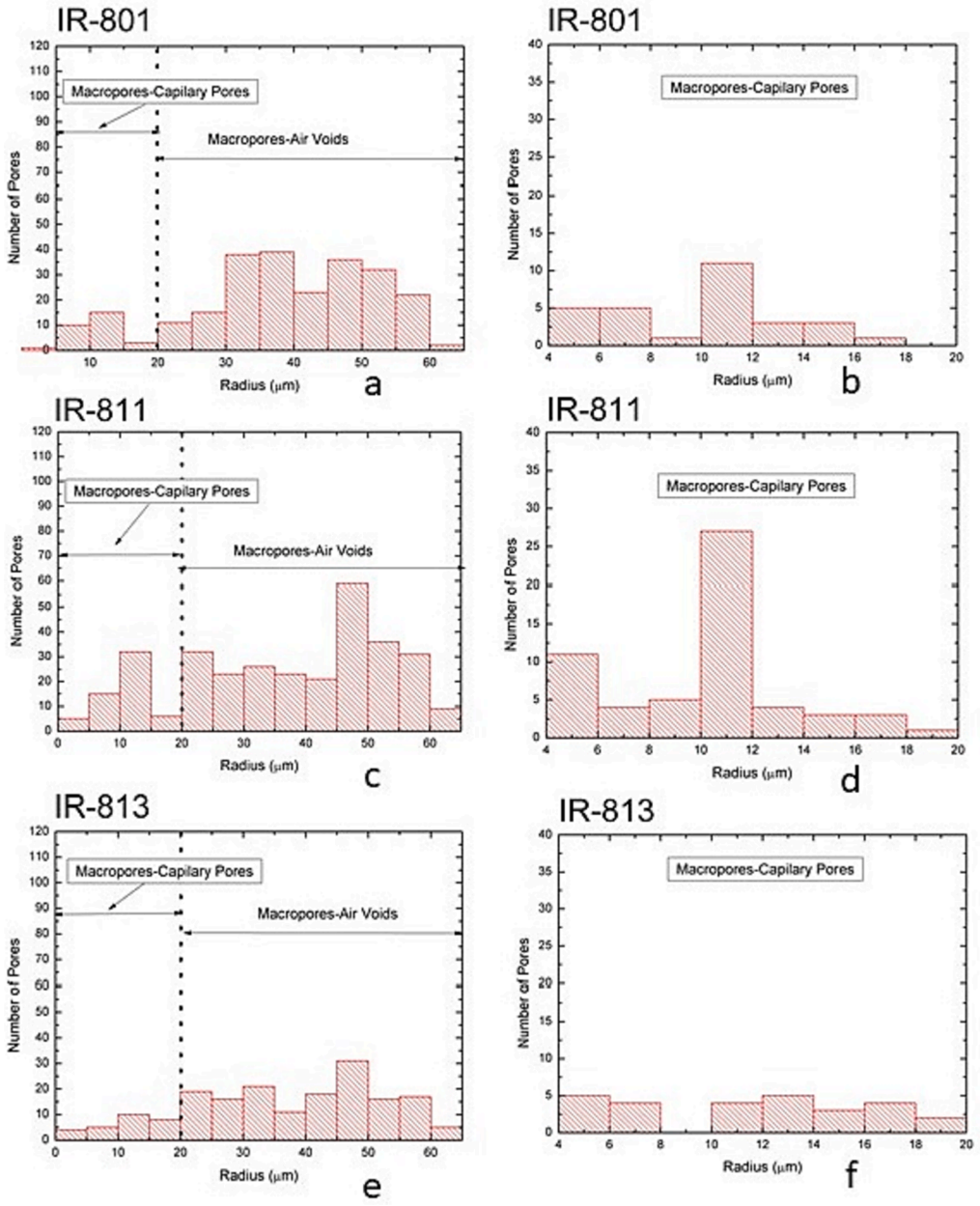

Fig. 6. Pore number (NP) distribution histograms of the IR samples.

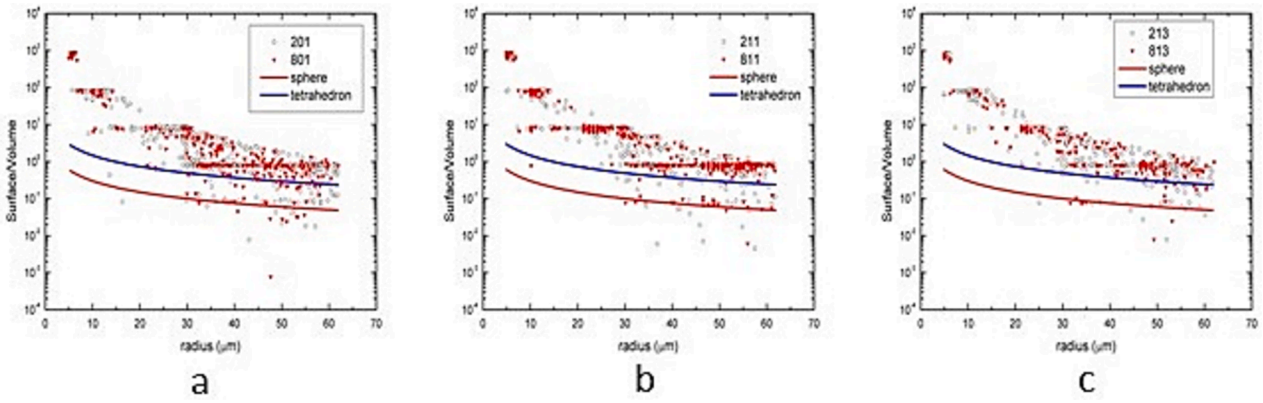

Fig. 7. Pore surface-volume ratio versus pore radius.

pores) present values between 1000 and 10, indicating high fractality. In addition, the air voids (radius greater than 20 μm) have low or even non-fractality due to the S-V ratio presents values lower than 10. The results suggest that samples submitted to sodium sulphate solution tend to have macropores with higher fractality than sample submitted to water and dry samples. We observed, through the simultaneous combination of diffraction and X-ray tomography results, that in saline conditions and/or when subjected to irradiation, the cement paste tends to become more mechanically fragile (increase in the number of macropores) for application in disposal facility, thus suggesting the need for more studies in order to minimize these effects.

Future studies can be developed to represent the complexity and interconnectivity of the pore networks and fracture systems. Other solution conditions, temperature variation and different irradiation exposure time need to be explored in order to comprise different possible environmental conditions, to associate mechanisms that affect material performance, concerning the radioactive waste repository facilities.

Declaration of Competing Interest

The authors declare that they have no known competing financial interests or personal relationships that could have appeared to influence the work reported in this paper.

Data availability

Data will be made available on request.

Acknowledgements

First and foremost, we would like to thank God, who has ensured knowledge and opportunities for the authors to complete this publication. The authors are grateful to Helmholtz Zentrum-Berlin (HZB)-BESSY for the opportunity to perform the experiment described in this study.

References

[1] INTERNATIONAL ATOMIC ENERGY AGENCY. Long term behavior of low and intermediate level waste packages under repository conditions. Results of a coordinated research project. TECDOC1397. Vienna, 2004.
[2] INTERNATIONAL ATOMIC ENERGY AGENCY. Predisposal Management of Radioactive Waste for protecting people and the environment. No. GSR Part 5. General Safety Requirements Part 5. Vienna, 2009.
[3] INTERNATIONAL ATOMIC ENERGY AGENCY, Scientific and Technical Basis for the Near Surface Disposal of Low and Intermediate Level Waste, Technical Reports Series No. 412, IAEA, Vienna, 2002.
[4] INTERNATIONAL ATOMIC ENERGY AGENCY. The behaviors of cementitious materials in long term storage and disposal of radioactive waste. Results of a Coordinated Research Project. IAEA-tecdoc-1701 Vienna, 2013.
[5] J.M. Galíndez, J. Molinero, Assessment of the long-term stability of cementitious barriers of radioactive waste repositories by using digital-image-based microstructure generation and reactive transport modelling, Cement and Concrete Research 40 (8) (2010) 1278–1289.
[6] X. Jiang, S. Mu, J. Liu., Influence of chlorides and salt concentration on salt crystallization damage of cement-based materials. Journal of Building Engineering, 61(2022),105260.
[7] C. Liu, J. Gao, F. Chen, Y. Zhao, X. Chen, Z. He, Coupled effect of relative humidity and temperature on degradation of cement mortars partially exposed to sulfate attack, Construction Build. Materials 216 (2019) 93–100.
[8] H.N. Atahan, K.M. Arslan, Improved durability of cement mortars exposed to external sulfate attack: The role of nano & micro additives, Sustainable Cities and Society 22 (2016) 40–48.
[9] F.P. Glasser, J. Marchand, E. Samson, Durability of concrete degradation phenomena involving detrimental chemical reactions, Cement Concrete Research 38 (2008) 226–246.
[10] INTERNATIONAL ATOMIC ENERGY AGENCY. Borehole disposal facilities for radioactive waste. IAEA SAFETY STANDARDS SERIES No. SSG-1, Vienna, 2009.
[11] ABNT NBR 11578,1997-Cimento Portland composto, Rio de Janeiro: Associação Brasileira de Normas Técnicas.
[12] ABNT NBR 7214, 2015 -Areia normal para ensaio de cimento – Rio de Janeiro: Associação Brasileira de Normas Técnicas, 2015.
[13] F.G. Moreno, C. Jiménez, P.H. Kamm, M. Klaus, G. Wagener, J. Banhart., Ch. Genzel, Qhite-beam, X-ray radioscopy and tomography with simultaneous diffraction at the EDDI beamline. J. Synchrotron Radiation. 20, 809-810. J.Appl. Cryst., 51(2013), 210-218. doi.org/10.1107/S1600576718000183.
[14] A.A. Coelho, TOPAS and TOPAS-Academic: an optimization program integrating computer algebra and crystallographic objects writtem in C++, 2018.
[15] , P. Bouniol, E. Bjergbakke, A comprehensive model to describe radiolytic processes in cement medium. Journal of Nuclear Materials, 372(2008), n. 1, 1–15.
[16] P. Bouniol, The influence of iron on water radiolysis in cement-based materials. Journal of Nuclear Materials, 403(2010), n. 1–3, 167–183.
[17] F. Vodák, K. Trtík, V. Sopko, O. Kapicková, P. Demo, Effect of γ-irradiation on strength of concrete for nuclear-safety structures. Cement and Concrete Research, 35(2005), n. 7, 1447–1451.
[18] G. Bar-nes, A Katz, Y. Peled, Y. Zeiri, The Combined Effect of Radiation and.
[19] Carbonation on the Immobilization of Sr and Cs Ions in Cementitious Pastes. Materials and Structures, 41(2008), n. 9, 1563–1570.
[20] J. W Bullard, H. M. Jennings, R. A. Livingston, A. Nonat, G.W. Scherer, J. S. Schweitzer, K. L. Scrivener, J. J. Thomas, Mechanisms of cement hydration. Cement and Concrete Research, 41(2011a), n. 12, 1208–1223.
[21] L. Nicoleau, A. Nonat, D. Perrey, The di- and tricalcium silicate dissolutions. Cement and Concrete Research, 47(2013), 14–30.
[22] M. Collepardi. A state-of-the-art review on delayed ettringite attack on concrete. Cement and Concrete Composites, 25(2003), n. 4–5, 401–407.
[23] P. Pipilikaki, M. Katsioti, J. L. Gallias, Performance of Limestone Cement Mortars in a High Sulfates Environment. Construction and Building Materials, 23(2009), n.2, 1042–1049.
[24] N. Mavropoulou, N. Katsiotis, J. Giannakopoulos, K. Koutsodontis, D. Papageorgiou, E. Chaniotakis, M. Katsioti, P.E. Tsakiridis, Durability Evaluation of Cement Exposed to Combined Action of Chloride and Sulphate Ions at Elevated Temperature: The Role of Limestone Filler, Construction and Building Materials 124 (2016) 558–565.
[25] K. Aligizaki, Pore Structure of Cement-Based Materials, 1st ed., Taylor & Francis, New York, 2006.
[26] J.F. Young, S. Mindess, A. Bentur, R.J. Gray, The Science and Technology of Civil Engineering Materials, Prentice Hall, Engelwood Cliffs, NJ, 1998.
[27] E.G.A. Ferreira, F. Yokaichiya, J.T. Marumo, R. Vicente, F. Garcia-Moreno, P. H. Kamm, M. Klaus, M. Russina, G. Gunther, C.E. Jimenez, M.K.K.D. Franco, Influence of the irradiation in cement for the Brazilian radioactive waste repositories: Characterization via X-ray diffraction, X-Ray Tomography and Quasielastic Neutron Scattering, Physica b: Physics of Condensed Matter 551 (2018) 256–261, https://doi.org/10.1016/j.physb.2018.01.018.